

Cite this: *Dalton Trans.*, 2017, **46**, 12425Received 17th July 2017,
Accepted 23rd August 2017

DOI: 10.1039/c7dt02597a

rsc.li/dalton

A new family of clusters containing a silver-centered tetracapped $[\text{Ag}@\text{Ag}_4(\mu_3\text{-P})_4]$ tetrahedron, inscribed within a N_{12} icosahedron†

Alexander V. Artem'ev,^a Irina Yu. Bagryanskaya,^{b,c} Evgeniya P. Doronina,^d
Peter M. Tolstoy,^e Artem L. Gushchin,^{a,c} Mariana I. Rakhmanova,^a
Alexander Yu. Ivanov^e and Anastasiya O. Suturina^d

An unprecedented silver-centered P-tetracapped $[\text{Ag}@\text{Ag}_4(\mu_3\text{-P})_4]$ tetrahedron inscribed within a N_{12} icosahedral cage has been discovered in the novel family of luminescent clusters. The latter are easily self-assembled by reacting Ag^{I} salts with tris(2-pyridyl)phosphine (Py_3P).

Currently, silver(I) complexes and clusters attract considerable attention because of their intriguing structural, photophysical, catalytic and biological properties.¹ One of the most powerful approaches to the synthesis of well-defined silver(I) clusters is self-assembly² from Ag^+ ions and diverse ligands such as N-heterocycles,³ carboxylates,⁴ sulfides and selenides,⁵ 1,1-dithiolates,⁶ and alkynyl anions.⁷ Among a plethora of ligands that are used for this purpose, phosphines containing additional donor sites are of special interest because they allow assembling a number of unique architectures.⁸ For instance, based on diphenyl-2-pyridylphosphine (dppy), a series of highly luminescent heterometallic Ag/Au clusters have been synthesized, e.g. $[\text{Au}_3(\text{E})\text{Ag}(\text{dppy})_3]^{2+}$,⁹ $[(\text{CCN})_2\text{Au}_8\text{Ag}_4(\text{dppy})_8(\text{MeCN})_2]^{6+}$,¹⁰ and $[\text{RCOAu}_4\text{Ag}_4(\text{dppy})_4]^{5+}$.¹¹ Recently,¹² using bis(2-pyridyl)phenylphosphine, the original 1D polymer $[\text{Ag}_2(\text{PPhPy}_2)_2\cdots\text{Cl}^-\cdots\text{Ag}_2(\text{PPhPy}_2)_2]_n$ has been

designed. Also, it is pertinent to note that silver(I) complexes with pyridylphosphines are prospective antitumour agents.¹³

Herein, we report on a new family of luminescent Ag(I) clusters with an unprecedented core structure, which can be viewed as a silver-centered phosphorus-tetracapped tetrahedron $[\text{Ag}@\text{Ag}_4(\mu_3\text{-P})_4]$, inscribed within a N_{12} icosahedral cage. These clusters have been readily self-assembled by reacting silver(I) salts with tris(2-pyridyl)phosphine under mild conditions. The photophysical and electrochemical properties as well as the electronic structure of the novel complexes have also been investigated.

We have discovered that tris(2-pyridyl)phosphine easily reacts with AgOTf in a 4 : 5 molar ratio (room temperature, $\text{CH}_2\text{Cl}_2/\text{MeCN}$, 1 h) to afford the unprecedented cluster $[\text{Ag}@\text{Ag}_4(\text{Py}_3\text{P})_4(\text{OTf})_4](\text{OTf})$ (**1**) in 84% yield (the synthetic details are in the ESI†). It is noteworthy that the variation of the reactant molar ratio (e.g. $\text{Ag}/\text{L} = 1 : 1$, $2 : 1$, $1 : 2$ or $2 : 3$) does not lead to the formation of other clusters apart from **1**. X-Ray diffraction (XRD) analysis reveals that this compound crystallizes from acetone solution as the $1.4\text{Me}_2\text{CO}$ solvate. The $[\text{Ag}@\text{Ag}_4(\text{Py}_3\text{P})_4(\text{OTf})_4]^+$ cation of the latter (Fig. 1a) contains a structurally remarkable $[\text{Ag}@\text{Ag}_4(\mu_3\text{-P})_4]$ skeleton which is best described as a C_3 -symmetrical Ag-centered Ag_4 tetrahedron ($\tau_4 = 0.954$ (ref. 14)) whose each triangular face is capped by a phosphorus atom ($\mu_3\text{-P}$) of the Py_3P ligands (Fig. 1b). Overall, the $[\text{Ag}@\text{Ag}_4(\mu_3\text{-P})_4]$ core is inscribed within a N_{12} icosahedron, constituted by the twelve pyridine nitrogen atoms of four Py_3P ligands. The central Ag atom has a slightly distorted P_4 tetrahedral environment ($\tau_4 = 0.984$ (ref. 14)), constituted by the four P atoms of the Py_3P ligands $[\text{Ag}-\text{P}, 2.5766(16) - 2.6095(15) \text{ \AA}]$. Each vertex Ag atom shows three short bonds with the N atoms of the three neighbouring Py_3P ligands $[\text{Ag}-\text{N}, 2.272(5) - 2.306(5) \text{ \AA}]$ and a one longer bond with a triflate O atom, thus adopting a $[3 + 1]$ trigonal pyramidal geometry. The three Ag–O bond lengths are similar (ca. 2.620 \AA), which suggests a weak association of the triflate anions with the Ag3, Ag4 and Ag5 atoms, whereas the Ag1–O3 distance $[2.7400(53) \text{ \AA}]$ is clearly non-bonded. The $\text{Ag}_{\text{central}} -$

^aNikolaev Institute of Inorganic Chemistry, Siberian Branch of Russian Academy of Sciences, 3, Akad. Lavrentiev Ave., Novosibirsk 630090, Russia.
E-mail: chemisufarm@yandex.ru

^bN. N. Vorozhtsov Novosibirsk Institute of Organic Chemistry, Siberian Branch of Russian Academy of Sciences, 9, Akad. Lavrentiev Ave., Novosibirsk 630090, Russia
^cNovosibirsk State University, National Research University, Department of Natural Sciences, 2, Pirogova Str., Novosibirsk 630090, Russia

^dA. E. Favorsky Irkutsk Institute of Chemistry, Siberian Branch of the Russian Academy of Sciences, 1 Favorsky Str., 664033 Irkutsk, Russia

^eSt. Petersburg State University, Center for Magnetic Resonance, Universitetskij pr. 26, St. Petersburg 198504, Russia

†Electronic supplementary information (ESI) available: Synthetic procedures, characterization data, NMR and FT-IR spectra, photophysical and electrochemical data, computation details. CCDC 1472281, 1472282, 1532341 and 1538903. For ESI and crystallographic data in CIF or other electronic format see DOI: 10.1039/c7dt02597a

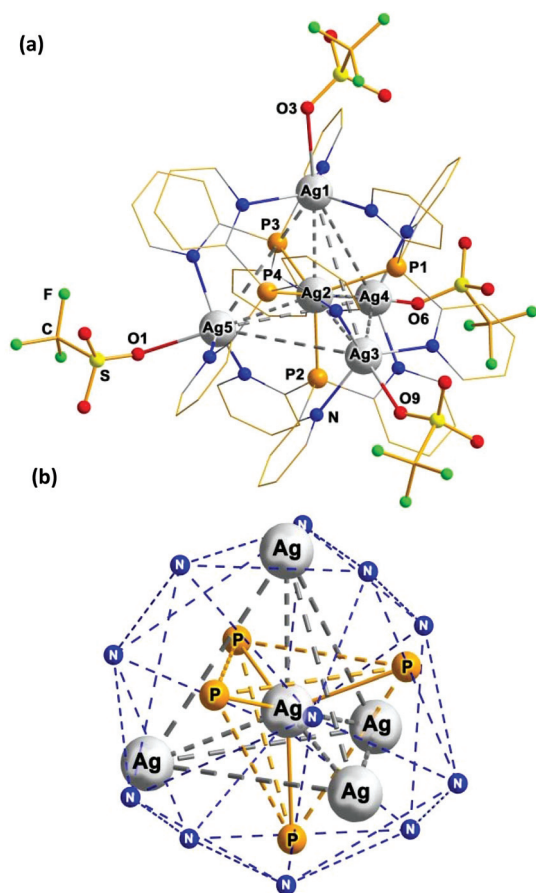


Fig. 1 (a) The structures of the $[\text{Ag}@\text{Ag}_4(\text{Py}_3\text{P})_4(\text{OTf})_4]^+$ core of $1\cdot 4\text{Me}_2\text{CO}$ (the pyridine H atoms are omitted for clarity). (b) Ag-centered P-tetracapped tetrahedron, $[\text{Ag}@\text{Ag}_4(\mu_3\text{-P})_4]$, inscribed in a N_{12} icosahedral cage. Selected bond lengths [Å]: Ag(1)–Ag(2) 3.1622(6), Ag(2)–Ag(4) 3.0917(7), Ag(2)–Ag(5) 3.1313(6), Ag(2)–Ag(3) 3.1638(6), Ag(1)–O(3) 2.7400(53), Ag(3)–O(9) 2.6229(53), Ag(4)–O(6) 2.6675(47), Ag(5)–O(1) 2.5711(56), Ag–P (av.) 2.593, Ag–N (av.) 2.288.

$\text{Ag}_{\text{vertex}}$ distances are quite short ranging from 3.0917(7) to 3.1638(6) Å [*cf.* with twice the van der Waals radius of Ag, 3.4 Å]. Meanwhile, the Ag–Ag distances along the edges of the Ag_4 tetrahedron are too long [5.0031(7)–5.2553(7) Å] for any argentophilic interactions. Thus, each Py_3P ligand binds the central metal (*via* the P atom) and the three adjacent $\text{Ag}_{\text{vertex}}$ ions (*via* pyridine N donors), exhibiting a P,N,N',N'' -coordination pattern.

The $[\text{Ag}@\text{Ag}_4(\text{Py}_3\text{P})_4]$ core of **1** is chiral due to a propeller-like arrangement of the pyridine cycles around four vertex silver atoms. Interestingly enough, exclusively $\Delta\Delta\Delta\Delta$ - and $\Lambda\Lambda\Lambda\Lambda$ -helical isomers are found in the packing of **1** (Fig. S1†), *i.e.* the $\text{Ag}_{\text{vertex}}$ atoms in each stereoisomer have an identical configuration.

Encouraged by the first result, we next have examined whether the disclosed approach could be used for the assembly of similar aggregates from other silver(I) salts. The experiments have shown that $[\text{Ag}(\text{MeCN})_4]\text{BF}_4$ and $[\text{Ag}(\text{MeCN})_4]\text{PF}_6$ interact with Py_3P in the same way to afford structurally related

clusters, $[\text{Ag}_4(\text{Ag})(\text{Py}_3\text{P})_4](\text{BF}_4)_5$ (**2**) and $[\text{Ag}_4(\text{Ag})(\text{Py}_3\text{P})_4](\text{PF}_6)_5$ (**3**), in 99 and 86% yield, respectively.† The data of elemental analysis, ^1H NMR and FT-IR spectroscopy of samples **2** and **3** confirm the above-mentioned formulations. The diffusion of hexane into a solution of **2** in an acetone/MeCN mixture results in X-ray quality crystals, the asymmetric unit of which consists of two cations, $[\text{Ag}@\text{Ag}_4(\text{Py}_3\text{P})_4(\text{Me}_2\text{CO})(\text{MeCN})_3]^{5+}$ (Fig. 2a) and suchlike $[\text{Ag}@\text{Ag}_4(\text{Py}_3\text{P})_4(\text{Me}_2\text{CO})(\text{MeCN})_2]^{5+}$ (Fig. S2†) along with ten BF_4^- anions. Similarly, the equal number of $\Delta\Delta\Delta\Delta$ - and $\Lambda\Lambda\Lambda\Lambda$ -enantiomers for both the cations is presented in the centrosymmetric crystals of **2**. On the whole, the $[\text{Ag}@\text{Ag}_4(\text{Py}_3\text{P})_4]$ skeleton **2** is almost superimposable with that of **1** (see the overlay of these fragments in Fig. S4†). One of the $\text{Ag}_{\text{vertex}}$ atoms of **2** is additionally ligated by O from acetone, whereas the remaining $\text{Ag}_{\text{vertex}}$ atoms are weakly bonded with MeCN molecules (Fig. 2a and S2†). At that, two basal atoms, Ag8 and Ag9, have quite similar Ag–N distances (2.542 and 2.550 Å), whereas the corresponding bond for Ag6 is somewhat longer: 2.681 Å.

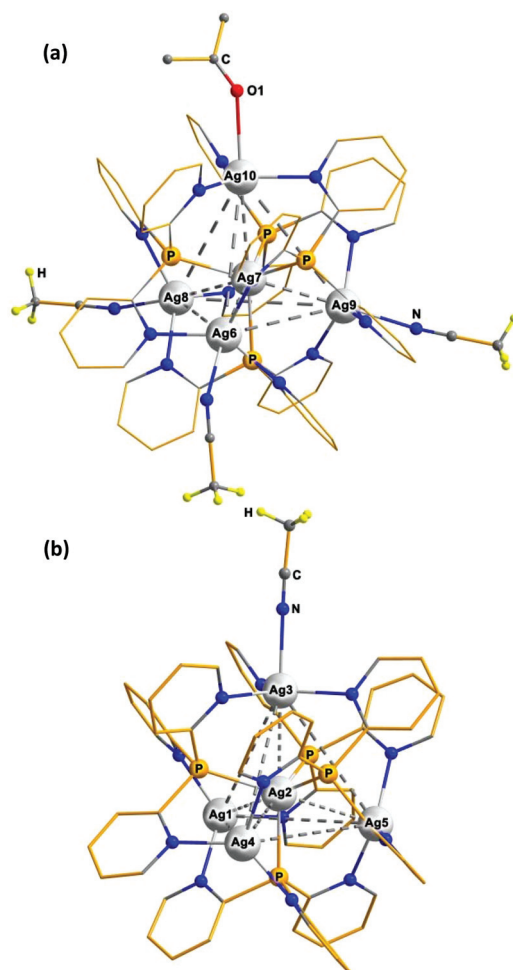


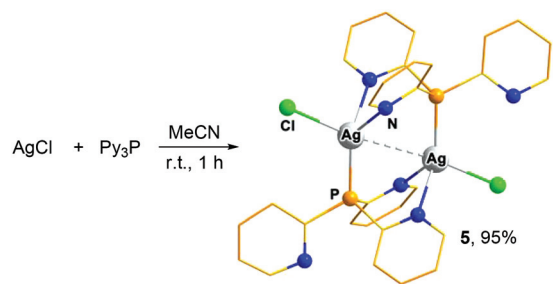
Fig. 2 The structures of the $[\text{Ag}@\text{Ag}_4(\text{Py}_3\text{P})_4(\text{Me}_2\text{CO})(\text{MeCN})_3]^{5+}$ (a) and $[\text{Ag}@\text{Ag}_4(\text{Py}_3\text{P})_4(\text{MeCN})]^{5+}$ (b) cations in **2**· $\text{Me}_2\text{CO}\cdot 2.5\text{MeCN}$ and **3**·MeCN, correspondingly (the pyridine H atoms are omitted for clarity).



The crystals of $[\text{Ag}@\text{Ag}_4(\text{Py}_3\text{P})_4(\text{MeCN})](\text{PF}_6)_5 \cdot 3\text{MeCN}$ have been obtained by diffusion of diethyl ether into an MeCN solution of **3**. XRD analysis revealed (Fig. 2b) that the $[\text{Ag}@\text{Ag}_4(\text{Py}_3\text{P})_4]$ unit in $[\text{Ag}@\text{Ag}_4(\text{Py}_3\text{P})_4(\text{MeCN})]^{5+}$ is nearly the same as that in **1** (Fig. S5†). As in the case in **2**, the PF_6^- anions of **3** remain non-coordinated. Therefore, the three basal Ag atoms are saturated by pyridyl N donors in a trigonal planar manner, while the fourth Ag centre (Ag3) is additionally ligated by a MeCN solvent molecule (Ag–N 2.497 Å).

Significantly, using two different Ag(I) salts in the reaction with Py_3P allows $[\text{Ag}@\text{Ag}_4(\text{Py}_3\text{P})_4]$ clusters bearing two types of counterions to be synthesized. So, we have found that $[\text{Ag}(\text{MeCN})_4]\text{PF}_6$ and four equivalents of $[\text{Ag}(\text{MeCN})_4]\text{BF}_4$ may be easily self-assembled into the pentanuclear cluster $[\text{Ag}_4(\text{Ag})(\text{Py}_3\text{P})_4](\text{PF}_6)(\text{BF}_4)_4$ (**4**) in 85% yield by the addition of four equivalents of Py_3P .† From the MeCN/Et₂O system, cluster **4** crystallizes as solvate 4·6MeCN containing $[\text{Ag}@\text{Ag}_4(\text{Py}_3\text{P})_4(\text{MeCN})_4]^{5+}$ cations (Fig. 3), the core of which is comparable to that of **1–3** (Fig. S6†).

Our attempts to obtain a similar polynuclear cluster using AgCl in reaction with Py_3P in a 5 : 4 molar ratio lead to the isolation of the dinuclear complex $[\text{Ag}(\text{Cl})(\mu\text{-Py}_3\text{P})_2]$ (**5**) in quantitative yield (Scheme 1, the synthetic details, and structural and luminescence properties are given in the ESI†). According to the XRD study, two Ag atoms in **5** are bridged by two Py_3P ligands in a head-to-tail fashion so that each metal coordinates two N atoms and one P atom from two adjacent ligands (Scheme 1 and Fig. S3†). Note that complexes of a similar structure, but with the PhPy_2P ligand, were previously described.^{12,15} The Ag–Ag distances in both independent molecules of **5** [3.2615(8) and 3.2701(9) Å] imply argentophilic interactions. In the solid state, this cluster exhibits blue-green emission ($\lambda_{\text{max}} = 500$ nm, Fig. S30†) with the modest PLQY (8% at 298 K).†



Scheme 1 Synthesis of dinuclear cluster **5**.

The pentanuclear clusters obtained are air- and light-stable powders and show good solubility in acetonitrile. All these clusters exhibit a high stability in solutions and can be recrystallized from them. The ESI-mass spectra of the clusters exhibit a number of low intensive peaks assigned to polynuclear Ag-containing species, thus indicative of a fragmentation of the $[\text{Ag}_4(\text{Ag})(\text{Py}_3\text{P})_4]^{5+}$ cation under ESI-conditions.

The NMR data reveal that the cluster cations of **1–4** remain intact in the solution state. So, in the $^{31}\text{P}\{^1\text{H}\}$ NMR spectrum of **1** dissolved in CD_3CN at 298 K, only one signal is visible at *ca.* 14.6 ppm with a large doublet splitting due to the $^{31}\text{P}_{-109/107}\text{Ag}$ coupling. The magnitude of this coupling (238 Hz for $^{31}\text{P}_{-109}\text{Ag}$ and 207 Hz for $^{31}\text{P}_{-107}\text{Ag}$) clearly suggests that all four P atoms are bonded to the Ag atom.¹⁶ Moreover, couplings with other Ag atoms of the complex are resolved as well (see Fig. 4, top, for the spectra and assignment of the couplings; we have tentatively assigned all 6–7 Hz splittings to the $^2J(\text{P-Ag-Ag})$ couplings, assuming that they are similar in value and that the $^3J(\text{P-C-N-Ag})$ coupling is too small to be resolved). The high resolution constant time $^1\text{H},^{15}\text{N}$ -HMBC spectrum, shown in Fig. 4, bottom, further reveals the $^1J(^{15}\text{N},^{109/107}\text{Ag})$ and $^2J(^{15}\text{N},^{109/107}\text{Ag})$ couplings consistent with the structure of the complex, as well as the $^2J(^{31}\text{P},^{15}\text{N})$ coupling

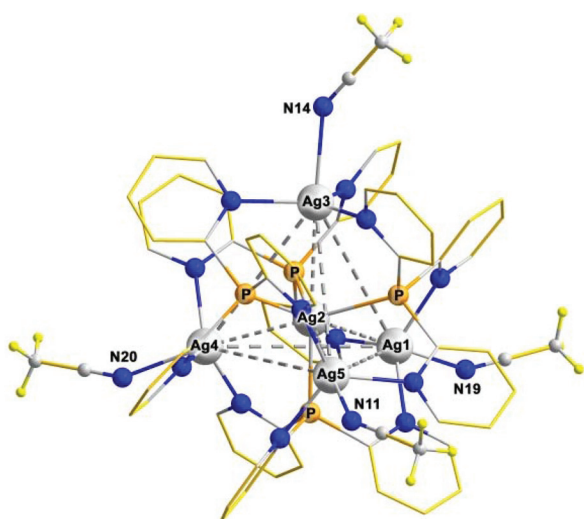


Fig. 3 The structures of the $[\text{Ag}@\text{Ag}_4(\text{Py}_3\text{P})_4(\text{MeCN})_4]^{5+}$ cation in 4·6MeCN, correspondingly (the pyridine H atoms are omitted for clarity).

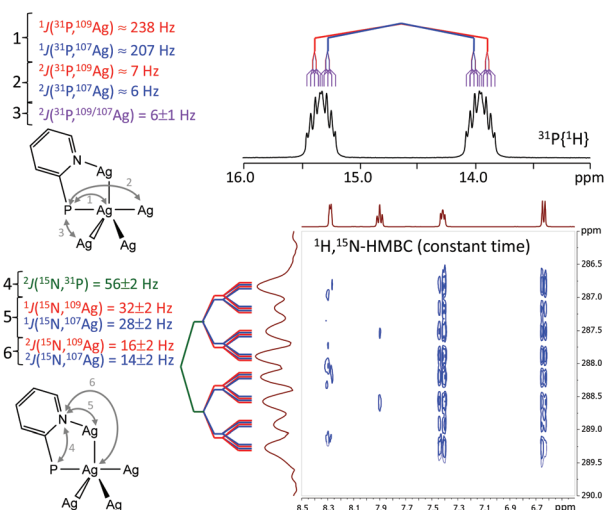


Fig. 4 $^{31}\text{P}\{^1\text{H}\}$ (top) and constant time $^1\text{H},^{15}\text{N}$ -HMBC (bottom) NMR spectra of **1** dissolved in CD_3CN at 300 K.



of ca. 56 Hz. Note that within the spectral line width the differences in couplings to ^{109}Ag and ^{107}Ag are not always resolved. The complete set of ^1H , $^{31}\text{P}\{^1\text{H}\}$, ^{109}Ag and lower resolution ^1H , ^{15}N -HMBC NMR spectra for complexes **1**, **2**, **3** and **4** dissolved in CD_3CN is given in the ESI (Fig. S7–S22†). The ^{109}Ag NMR signals of **1–4** do not show clear Ag–P splitting patterns. However, these signals have similar line shapes with a pedestal (see Fig. S9, S13, S17 and S21†) indicating the presence of some kind of splitting. At the given signal-to-noise ratio (up to 4 days of acquisition), it is hard to speculate about the number of signals and the types of spin systems. In turn, the signal of the central silver atom is not observed in the ^{109}Ag NMR spectra because it should be four times less intensive and additionally split into complicated multiplets due to the one-bond couplings with phosphorous and silver nuclei.

The UV-Vis spectra of clusters **1–4** are characterized by a strong band at 260 nm and a weak shoulder expanding from 275 to 340 nm (Fig. S29†). The high-energy band could be assigned to intraligand transitions because the Py_3P itself displays the same absorption. The weak band in the region 275–340 nm is tentatively assigned to metal-to-ligand charge transfer transitions that is in accordance with DFT calculations (*vide infra*).

The luminescence properties of clusters **1–4** have been preliminarily investigated in the solid state. All these exhibit a greenish-blue emission at room temperature with the quantum yields up to 24% (Table 1). The excitation and emission spectra of **1–4** are depicted in Fig. 5. Clusters **4**, **3**, **1** and **2**

Table 1 Photophysical properties of clusters **1–4** at 300 K

	$\lambda_{\text{max}}^{\text{ex}}$ (nm)	$\lambda_{\text{max}}^{\text{em}}$ (nm)	ϕ_{PL} (%)
1	350	490	14
2	360	510	24
3	350	480	18
4	350	470	2

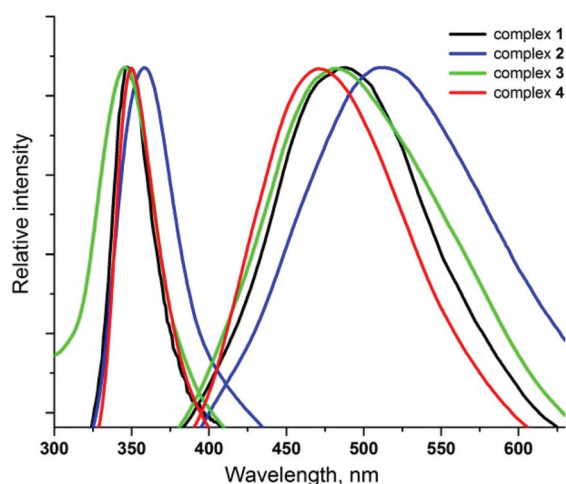


Fig. 5 Normalized excitation and emission spectra of **1–4** in powder states at 300 K.

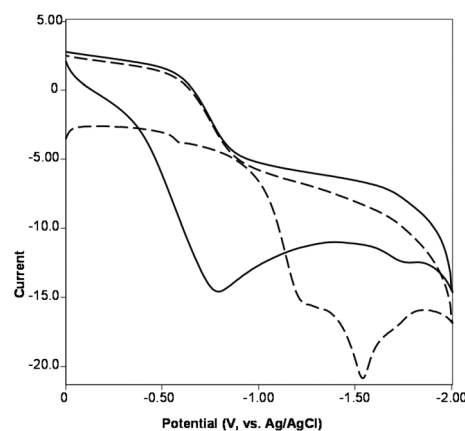


Fig. 6 CV of **1** in CH_3CN between $0 \leftrightarrow -2$ V at 0.1 V s^{-1} scan rate (dashed line is the first scan, solid line is the second scan).

show a broad emission with the maxima at 470, 480, 490 and 510 nm, respectively, *i.e.* the distinct red-shift of the emission maxima is observed in this range, while the free Py_3P displays a broad emission with λ_{max} at about 420 nm. Taking into account the literature data,^{3c} the origin of luminescence of **1–4** can be ascribed to metal-to-ligand charge transfer states, perturbed by the presence of $\text{Ag}\cdots\text{Ag}$ interactions.

The redox properties of clusters **1–4** have been investigated by cyclic voltammetry (CV). All compounds demonstrate similar redox behavior in the negative range (up to -2 V) and reveal irreversible reduction processes which can be assigned to the $\text{Ag}^{\text{I}}/\text{Ag}^0$ couple. The cathodic potential values (Table S3†) strongly depend on the number of scans and dramatically change on going from the first scan to the second one. In particular, the CV of **1** shows two cathodic peaks at -1.2 and -1.5 V (*vs.* Ag/AgCl) at the first scan which are further transformed to the broad wave centered at -0.77 V at the second scan (Fig. 6). This behavior can be explained by absorption of the reduction products on the surface of the working electrode.

Conclusions

In summary, we have presented the novel family of luminescent clusters containing a remarkable Ag-centered P-tetracapped tetrahedral $[\text{Ag}@\text{Ag}_4(\mu_3\text{-P})_4]$ unit inscribed within a N_{12} icosahedron. Taking into account the intriguing structure of these clusters and their facile and almost quantitative self-assembly from available reagents, one expects that the reported finding would stimulate intense research interest in this area. Further investigation of the silver clusters is in progress.

Conflicts of interest

There are no conflicts to declare.



Acknowledgements

The authors acknowledge the financial support from the Russian Foundation for Basic Research (Grant 15-03-05591). We also are grateful to Multi-Access Chemical Service Center SB RAS for XRD analysis. Supported by Russian Ministry of Science and Education under 5-100 Excellence Programme.

Notes and references

- (a) G. Fang and X. Bi, *Chem. Soc. Rev.*, 2015, **44**, 8124–8173; (b) S. Medici, M. Peana, G. Crisponi, V. M. Nurchi, J. I. Lachowicz, M. Remelli and M. A. Zoroddu, *Coord. Chem. Rev.*, 2016, **327–328**, 349–359; (c) H. Pellissier, *Chem. Rev.*, 2016, **116**, 14868–14917.
- S.-L. Zheng, M.-L. Tong and X.-M. Chen, *Coord. Chem. Rev.*, 2003, **246**, 185–202.
- (a) A. N. Khlobystov, A. J. Blake, N. R. Champness, D. A. Lemenovskii, A. G. Majouga, N. V. Zyk and M. Schröder, *Coord. Chem. Rev.*, 2001, **222**, 155–192; (b) P. J. Steel and C. M. Fitchett, *Coord. Chem. Rev.*, 2008, **252**, 990–1006; (c) E. M. Njogu, B. Omondi and V. O. Nyamori, *J. Coord. Chem.*, 2015, **68**, 3389–3431; (d) X.-P. Wang, T.-P. Hu and D. Sun, *CrystEngComm*, 2015, **17**, 3393–3417.
- (a) L. Brammer, M. D. Burgard, C. S. Rodger, J. K. Swearingen and N. P. Rath, *Chem. Commun.*, 2001, 2468–2469; (b) Q.-M. Wang and T. C. W. Mak, *J. Am. Chem. Soc.*, 2001, **123**, 7594–7600.
- (a) O. Fuhr, S. Dehnen and D. Fenske, *Chem. Soc. Rev.*, 2013, **42**, 1871–1906; (b) Y.-P. Xie, J.-L. Jin, G.-X. Duan, X. Lu and T. C. W. Mak, *J. Coord. Chem.*, 2017, **331**, 54–72.
- (a) J.-H. Liao, C. Latouche, B. Li, S. Kahlal, J.-Y. Saillard and C. W. Liu, *Inorg. Chem.*, 2014, **53**, 2260–2267; (b) R. S. Dhayal, J.-H. Liao, Y.-C. Liu, M.-H. Chiang, S. Kahlal, J.-Y. Saillard and C. W. Liu, *Angew. Chem., Int. Ed.*, 2015, **54**, 3702–3706; (c) R. S. Dhayal, Y.-R. Lin, J.-H. Liao, Y.-J. Chen, Y.-C. Liu, M.-H. Chiang, S. Kahlal, J.-Y. Saillard and C. W. Liu, *Chem. – Eur. J.*, 2016, **22**, 9943–9947.
- (a) Q.-M. Wang, Y.-M. Lin and K.-G. Liu, *Acc. Chem. Res.*, 2015, **48**, 1570–1579; (b) Y.-T. Chen, I. S. Krytchankou, A. J. Karttunen, E. V. Grachova, S. P. Tunik, P.-T. Chou and I. O. Koshevoy, *Organometallics*, 2017, **36**, 480–489.
- (a) M. Scheer, L. J. Gregoriades, A. V. Virovets, W. Kunz, R. Neueder and I. Krossing, *Angew. Chem., Int. Ed.*, 2006, **45**, 5689–5693; (b) S. L. James, *Chem. Soc. Rev.*, 2009, **38**, 1744–1758; (c) R. Meijboom, R. J. Bowen and S. J. Berners-Price, *Coord. Chem. Rev.*, 2009, **253**, 325–342.
- (a) Q.-M. Wang, Y.-A. Lee, O. Crespo, J. Deaton, C. Tang, H. J. Gysling, M. C. Gimeno, C. Larraz, M. D. Villacampa, A. Laguna and R. Eisenberg, *J. Am. Chem. Soc.*, 2004, **126**, 9488–9489; (b) J.-H. Jia and Q.-M. Wang, *J. Am. Chem. Soc.*, 2009, **131**, 16634–16635; (c) L.-Q. Mo, J.-H. Jia, L. Sun and Q.-M. Wang, *Chem. Commun.*, 2012, **48**, 8691–8693.
- X.-L. Pei, Y. Yang, Z. Lei and Q.-M. Wang, *J. Am. Chem. Soc.*, 2013, **135**, 6435–6437.
- X.-L. Pei, Y. Yang, Z. Lei, S.-S. Chang, Z.-J. Guan, X.-K. Wan, T.-B. Wen and Q.-M. Wang, *J. Am. Chem. Soc.*, 2015, **137**, 5520–5525.
- T. Zhang, C. Ji, K. Wang, D. Fortin and P. D. Harvey, *Inorg. Chem.*, 2010, **49**, 11069–11076.
- (a) S. J. Berners-Price, R. J. Bowen, P. J. Harvey, P. C. Healy and G. A. Koutsantonis, *J. Chem. Soc., Dalton Trans.*, 1998, 1743–1750; (b) J. J. Liu, P. Galettisa, A. Farr, L. Maharaja, H. Samarasingha, A. C. McGechan, B. C. Baguley, R. J. Bowen, S. J. Berners-Price and M. J. McKeage, *J. Inorg. Biochem.*, 2008, **102**, 303–310.
- L. Yang, D. R. Powell and R. P. Houser, *Dalton Trans.*, 2007, 955–964.
- O. Crespo, M. C. Gimeno, A. Laguna and C. Larraz, *Z. Naturforsch., B: Chem. Sci.*, 2009, **64**, 1525–1534.
- (a) S. J. B. Price, C. Brevard, A. Pagelot and P. J. Sadler, *Inorg. Chem.*, 1985, **24**, 4278–4281; (b) A. D. Zotto and E. Zangrando, *Inorg. Chim. Acta*, 1998, **277**, 111–117.

